FCI TEST RESULTS UNDER CONDITIONS OF PARTIALLY FLOODED CAVITY AND FLOODED REACTOR IN THE TROI

S.W. HONG [1)], Y.S Na, S. H. Hong and J. H. SONG
Korea Atomic Energy Research Institute
989-111 Daedeok-daero, Yuseong-gu, Daejon, 305-353, KOREA
[1)] swhong@kaeri.re.kr

ABSTRACT

The Korea Atomic Energy Research Institute (KAERI) has operated the TROI (Test for Real cOrium Interaction with water) facility for studies on fuel-coolant interactions (FCIs) since 2001. Before the OECD/SERENA project, which was commonly operated by the CEA and KAERI, and completed in 2012, the fuel coolant interaction tests using prototypic corium in facilities of the TROI in KAERI and the KROTOS in CEA were conducted to simulate a FCI under conditions in which a reactor cavity is partially flooded. Some advanced reactors such as APR1400 and AP1000 adapt the in-vessel retention concept by ex-vessel cooing. In this case, the molten corium in a reactor vessel is directly injected into the water in the reactor cavity without a free fall. KAERI has produced FCI data to simulate the conditions that the reactor vessel is fully flooded using ZrO2 and molten corium. In this paper, the results of the FCI experiment under reactor submerged conditions are compared with the FCI data produced under the conditions in which the reactor vessel is partially flooded.

KEYWORDS
FCI, Cavity, Rector, Submerged, Free Fall

1. INTRODUCTION

The Korea Atomic Energy Research Institute (KAERI) has conducted a TROI (Test for Real cOrium Interaction with water) program for studies on fuel-coolant interactions (FCIs) since 2001. More than 70 experiments using several prototypic materials have been carried out to observe the FCI phenomena conventionally of interest in TROI. In other words, molten material is injected into water in the interaction chamber passing a distance from the melt release location to the water surface of the interaction chamber to simulate a FCI under partially flooded reactor cavity conditions. In a TROI test, FCI tests under partially flooded reactor cavity conditions to see the effects of the composition, water subcooling, and water depth [1,2,3,4,5] were carried out. All FCI tests including OECD/NEA SERENA project [6] and KROTOS [7] were carried out under partially flooded reactor cavity conditions. However, the concluding remarks on the integrity of the reactor cavity by a steam explosion from the research under partially flooded reactor cavity conditions are still not clear and uncertain because of scalability with the real reactor scale from the experiments. Nevertheless, some advanced reactors such as APR1400 and AP1000 adapt the in-vessel retention concept by ex-vessel cooing. In this case, FCI occurs under fully flooded reactor conditions, so-called reactor submerged conditions, where molten material is injected into water without a free fall.

The premixing process is the first stage and has utmost importance to determine the subsequence of three-step events in the steam explosion. In the process of the premixing, the break-up length and fragmentation of the jet are important parameters to determine the premixing process. This paper briefly

provides information on the difference in the premixing process observed in the experiment between the partially flooded reactor cavity conditions and the reactor submerged conditions.

2. EXPERIMENTAL FACILITIES

Fig. 1 shows TROI experimental facility typically used in the test. The left one shows the facility used to simulate a partially flooded reactor cavity conditions, and the right one to the reactor submerged conditions. To simulate partially flooded reactor cavity conditions, molten material is released by gravity with a 1-m free fall, which is the distance from the exit of the intermediate melt catcher to the water surfaces, as shown in Fig. 1a. For reactor submerged conditions, the molten material is released into the water surface without a free fall, which is the distance from the exit of the intermediate melt catcher to the water surfaces, as shown in Fig. 1b. After the melt is produced and superheated sufficiently in the cold crucible, at the required melt temperature, a plug is removed and a puncher is actuated pneumatically. Then, the melt in the crucible is discharged by gravity and is accumulated in the intermediate melt catcher. The melt is delivered into the water in the interaction vessel by opening the slide valve of the intermediate melt catcher. The structure of the intermediate melt catcher is in Fig. 2. The left structure in Fig. 2 is used to simulate partially flooded reactor cavity conditions, and the right structure shows the reactor submerged conditions.

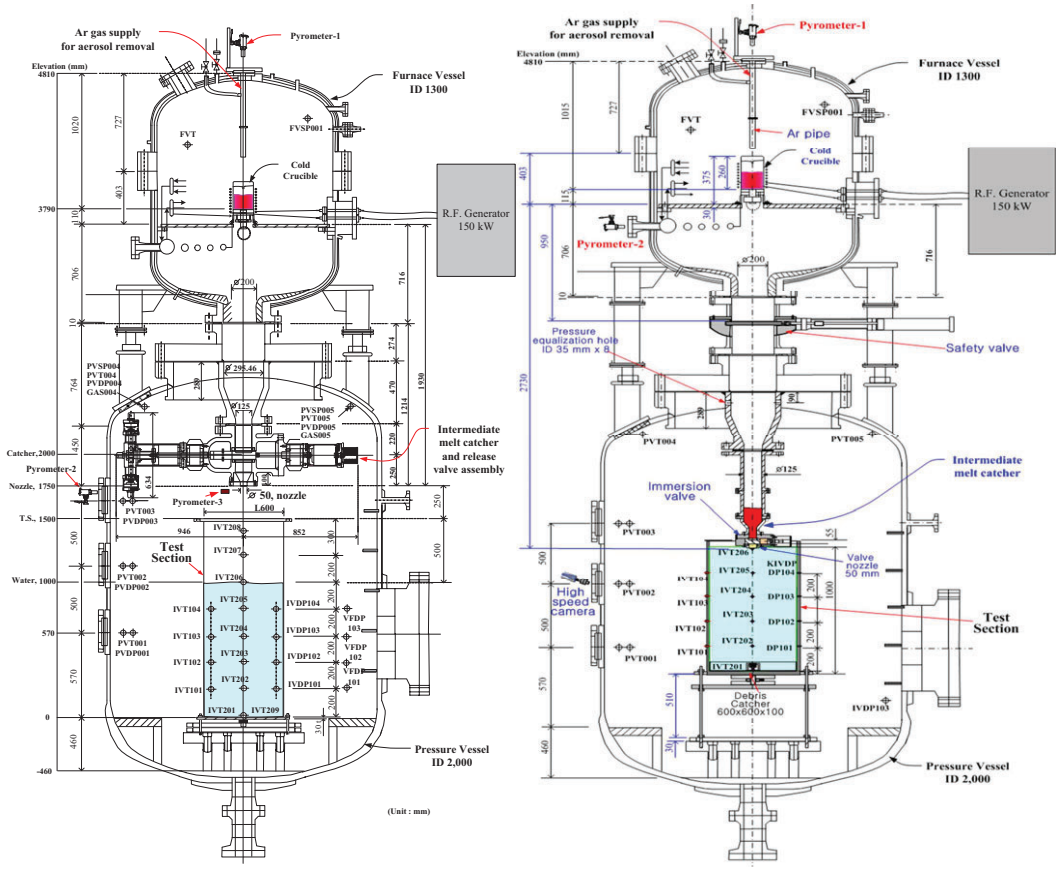

1a. For partially flooded reactor cavity 1b. For reactor submerged

Figure 1 TROI experimental facility

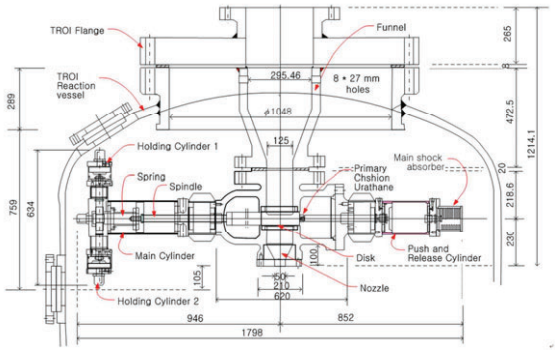

2a. For partially flooded reactor cavity

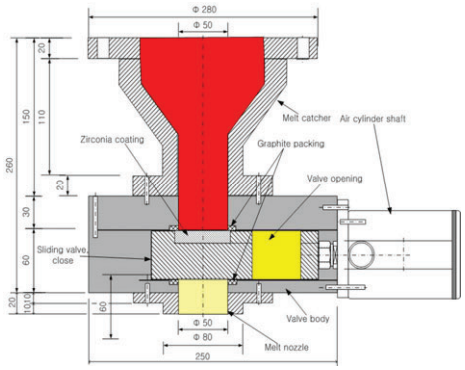

2b. For reactor submerged

Figure 2 Intermediate catcher

3. TEST RESULTS

3.1. Test Results Using ZrO2

The initial FCI conditions used to simulate a partially flooded reactor cavity and a submerged reactor are selected slightly differently, as shown in Table 2, because tests were not carried out for the direct comparison. However, some information such as the melt progression using high-speed visualization in water and the explosivity are comparable and informative for an understanding of the difference in the premixing process. A TROI-30 test was carried out in 2003 in the frame of the TROI program to visualize the melt progression in water. In this test, the melt is released without the intermediate catcher shown in (a) of Fig. 1. The melt is released at the bottom of the crucible and is injected into water after passing 3.8m by a gravitational fall. The melt jet diameter before the melt is injected into water is not known. The only available information of the melt jet diameter is the perforated size of the crust formed at the bottom of the crucible. This size is about 3cm. Thus, the melt jet diameter before melt injection into water is less than 3cm. The TROI76-W4 was carried out in 2013. In the TROI76-W4, the molten melt is directly injected into water without a free fall. In the tests, a square rectangular interaction chamber with an inner cross section of 60cm x 60cm is used to visualize the mixing zone and the melt front velocity in the water. The initial water levels during the TROI-30 test and TROI76-W4 test were 60 cm and 100 cm, respectively. The melt mass injected into the chamber was 2.98kg in the TROI-30 and 11.916kg in the TROI76-W4. The initial water temperatures were 284 and 341K, respectively.

A typical instrumentation sheet is shown in Table 1. More details are given in Ref. [6].

Table 1: Standard instrumentation of TROI test section
Origin of the transducer coordinates:

Radius (r, mm): From the test section (TS) centreline
Elevation (z, mm): From the bottom of the test section (TS)
Azimuth (θ, °): From the east

Transducer name	Position (r, z, θ)	Measured Quantity	Transducer Type	Range	Sampling time/ Acquisition duration	Comments
KIVDP101	300, 200, 80	Explosion pressure	Dynamic pressure transducer KISTLER 6005	0 – 100 MPa	0.01 ms/ 5 s	KIVDP's installed flushed to the inner wall of TS
KIVDP102	300, 400, 80					
KIVDP103	300, 600, 80					
KIVDP104	300, 800, 80					
PIVDP101	300, 200, 90	Explosion pressure	Dynamic pressure transducer PCB112A03	0 – 69 MPa	0.01 ms/ 5 s	PIVDP's installed flushed to the inner wall of TS
PIVDP102	300, 400, 90					
PIVDP103	300, 600, 90					
PIVDP104	300, 800, 90					
FVSP001	600, 4810, 0	Ambient pressure	Keller PA23S	0 – 1 MPa	30 ms/ 20 min	
PVSP004	800, 2360, 315					
PVSP005	800, 2360, 135					
IVT201	50, 0, 135	Melt front detection	Thermocouple K-Type 0.5 mm	1250°C	30 ms/ 20 min	
IVT202	0, 200, 0					
IVT203	0, 400, 0					
IVT204	0, 600, 0					
IVT205	0, 800, 0					
IVT206	0, 1000, 0					
IVT207	0, 1200, 0					
IVT208	0, 1400, 0					
IVT209	50, 0, 225					
IVT101	295, 200, 350	Water temperature	Thermocouple K-Type 0.5 mm	1250°C	30 ms/ 20 min	
IVT102	295, 400, 350					
IVT103	295, 600, 350					
IVT104	295, 800, 350					
PVT001	995, 570, 315	Free-board temperature	Thermocouple K-Type 0.5 mm	1250°C	30 ms/ 20 min	
PVT002	995, 1070, 315					
PVT003	995, 1570, 315					
PVT004	795, 2355, 315					
PVT005	795, 2355, 135					
FVT	740, 4360, 0					
VFDP101	300, 200-400, 0	Void fraction	Differential pressure transmitter Rosemount 3051S	200 mm H_2O	30 ms/ 20 min	Differential pressure to be converted to void fraction
VFDP102	300, 400-600, 0					
VFDP103	300, 600-800, 0					
HSC001	1100, 1570, 90	Jet visualization	Video camera Phantom		1000 f/s during 4 s	
HSC002	1100, 1570, 180					
MELTTEMP1	0, 4810, 0	Melt temperature	Pyrometer IRCON 3R-35C15-0-0-0-1	1500 – 3500°C	1 s / heating duration	
MELTTEMP2	1100, 1570, 270	Jet temperature	Pyrometer IRCON 3R-35C15-0-0-0-1	1500 – 3500°C	30 ms/ 20 min	
MELTTEMP3	100, 1570, 45	Jet temperature	Pyrometer IRCON 3R-35C15-0-0-0-1	1500 – 3500°C	30 ms/ 20 min	Fiber optics
IVDL101	0, -50, 0	Force	Force sensor KISTLER 9081A	0 - 650 kN	0.01 ms/ 5 s	
PVDP004	800, 2360, 315	Ambient dynamic pressure	Dynamic pressure transducer KISTLER 6061B	0 – 25 MPa	0.01 ms/ 5 s	
PVDP005	800, 2360, 135					

Table 2 Initial conditions

TROI test number	Unit	TROI30	TROI76-W4
Melt ZrO2/Zr	[w/o]	99.5/0.5	99.5/0.5
Temperature	[K]	Not Available	3040
Charged mass	[kg]	12.165	17.890
Released mass	[kg]	2.98	11.916
Plug/puncher diameter	[cm]	8.0/6.5	10.0/8.5
jet diameter	[cm]	< ~3.0 cm	5.0(nozzle)
Nozzle to water surface distance	[m]	3.8	-0.01
Test Section Water mass	[kg]	241	360
Water pool depth	[cm]	67	100
Cross section area	[m2]	0.36	0.36
Initial temperature	[K]	284	341
Pressure Vessel Initial pressure(air)	[MPa]	0.114	0.140
Initial temperature	[K]	286	311

Fig. 3 shows images taken by a high-speed camera in the TROI-30. The melt is injected into water at 1251ms after the operation of the puncher to perforate the crust formed at the bottom of the crucible and contacted with the bottom of the interaction chamber at 1792ms. It takes 0.54 sec for the melt front to pass through a water level of 67 cm. The average melt front velocity considering this time from the images is 1.23m/s. Fig. 4 shows the images taken by a high-speed camera in the TROI76-W4 just before the melt reached the bottom of the interaction chamber. The average velocity of the melt front passing through a 1m water pool is estimated using images. The average velocity of the melt front from the images is about 2.3 m/s, as shown in Fig. 4. A large bubble was observed on the surface of the mixing zone and went up. The size of the mixing zone is about 20 cm. This kind of information can be used for a code validation. Here, we may question why the melt propagation velocity in the case of a submerged melt release is higher than the one in the case of melt release when not submerged. One of the reasons may be that, for reactor submerged case, the melt stream is directly injected into the water without a break-up as a hot stick is injected into water, a large bubble surrounding the melt stream is generated, and the melt stream easily penetrates into the water because of the nearly free viscous state on the surface. However, in the case with a free fall, for the TROI30, the melt jet partly breaks up before the main melt jet comes into water and the mixing zone in front of the melt jet may consist of water, vapor, and melt drops. Accordingly, the main melt stream has to penetrate the viscous mixing zone and the velocity of main melt stream can be slower than the case where there is a free fall. This explanation is hypothetical, and not currently proved by the data.

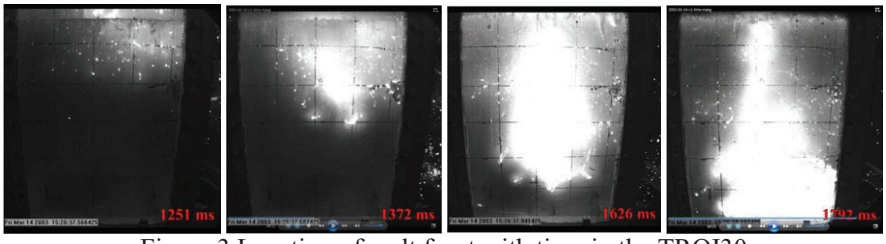

Figure 3 Location of melt front with time in the TROI30

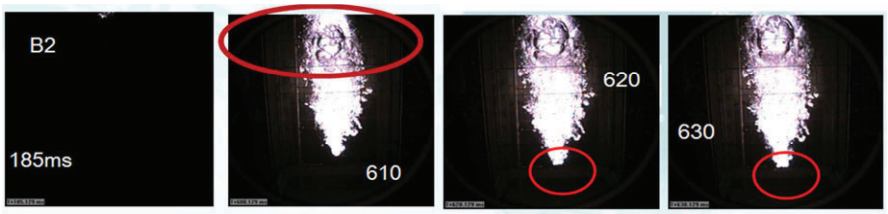

Figure 4 Location of melt front with time in the TROI76-W4

Fig. 5 shows the sensors and their location in the TROI30 tests. The information on the sensor types is in Table 1.

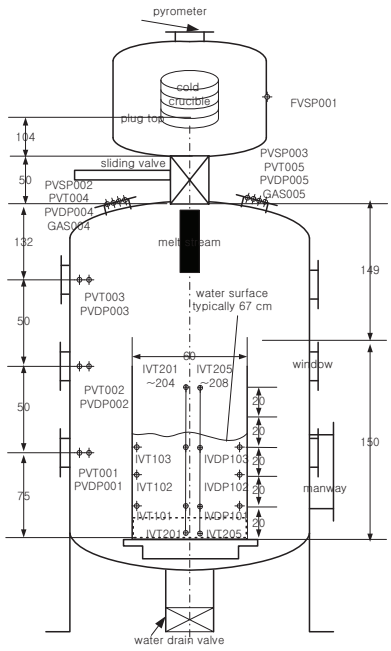

Figure 5. Measurement in the TROI30

Fig. 6 shows the time passing through the sacrificial thermocouples which are located in the center of the interaction chamber. The time at Fig. 6a is the time after the puncher operation. In the TROI-30, as shown in Fig. 6, IVT201 and IVT205 are located near the bottom of the debris-catcher and they indicate the time of the melt arrival at the bottom of the test section. The first indication of IVT201 and IVT205 is at about 6170.8 seconds, which is the time after the system operation by the PC has started. Thus, it took about 1.8 seconds after the actuation of the puncher. The thermocouples of IVT202 and IVT206 are located 20 cm above the locations of IVT201 and IVT205, as shown in Fig. 6. The distance between IVT203 and IVT202 is 40 cm. The thermocouples IVT204 and IVT208 are located 40 cm above the thermocouples IVT203 and IVT207. The melt jet passed the thermocouple IVT203 at about 1.1 second; IVT202, at 1.5 second; and IVT201, at 1.8 second. Thus, the melt jet velocity is about 0.6 m/s between IVT203 and IVT202, and 1.0 m/s between IVT202 and IVT201. Therefore, the melt jet velocity in the pool is between 0.6 and 1.0 m/s. The signals from the thermocouples of IVT204 and IVT208 are different from those of other thermocouples because they are exposed to the air. Thus, the radiation heat due to the melt jet at very high temperature affects the thermocouple.

The time in Fig. 6b is the time after opening the sliding valve of the intermediate catcher of (b) of Fig. 1. The level in 6b of Fig. 6 is the distance from the bottom of the interaction chamber. The melt front passes 1m from the bottom of the interaction at 0.27sec and 0.6m at 0.45sec, as shown in Fig. 6b. The average melt front velocity for this span is 2.2 m/s. This value is almost the same as 2.3 m/s, as estimated from the images taken by a high speed camera in the previous paragraph. It is estimated that the blue line located at 0.4m does not provide useful information because the melt front touches at about 0.63s. Sometimes, a thermo couple is not touched by the melt front because the melt front is not symmetric.

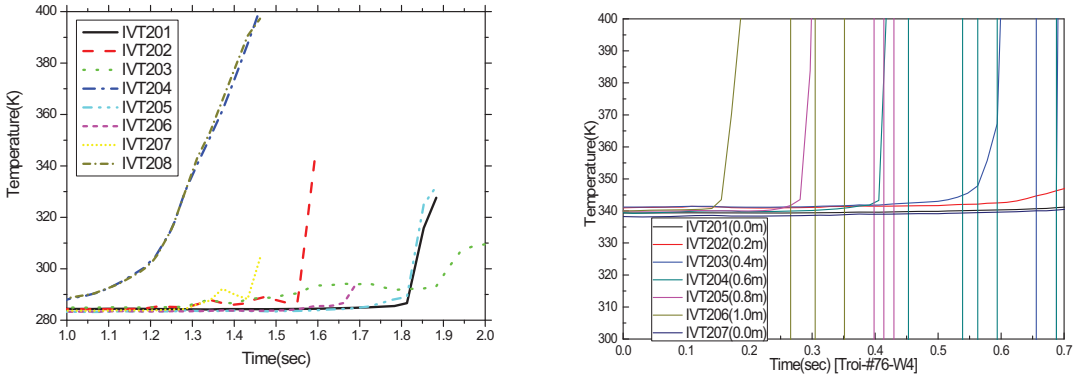

6a. TROI30 6b. TROI76-W4

Figure 6. Time passing sacrificial thermocouples

In the TRO30, the time for the puncher actuation is 6168.943 seconds and puncher actuation triggers the dynamic data acquisition. Then, second 0 of the above x-axis means the puncher actuation 6168.943 seconds after starting the melt. An explosion occurred at 1.8 seconds after the puncher actuation, and the melt jet arrived at the bottom at this time, as shown in Fig. 7a. Thus, the triggering might occur owing to the contact of the melt jet to the bottom. The explosion peak pressure is 5.5Mpa and its duration is 5 milliseconds. In the TROI76-W4 test, no dynamic pressure was detected, as shown in Fig. 7b, because there was no steam explosion.

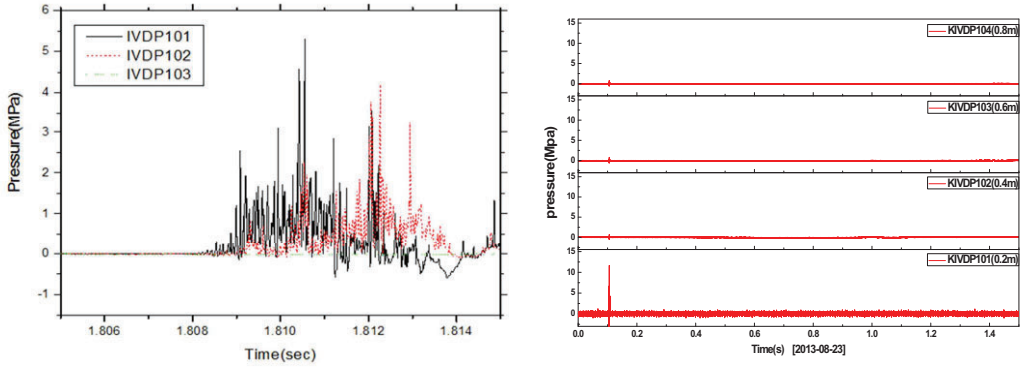

7a. TROI30 7b. TROI76-W4

Figure 7. Dynamic Pressure

In the TROI-30, the void fraction measurement system using the differential pressure sensors was not applied. However, the analysis of the water level swell at the time the steam explosion occurred using images from a high-speed camera shows that the volume average void fraction is around 10% because the level swell just before the triggering is about 6cm. The volume average void fraction is measured using the differential pressure sensors in the TROI76-W4. In the TROI76-W4, the maximum void fraction during the period the melt reaches the bottom of the interaction chamber is about 6% at about 5.5 sec, as shown in Fig 8a. The maximum void fraction from 1.2 sec to 1.6 sec after the melt touches the bottom of the interaction chamber, as shown in Fig 8b, is about 60%.

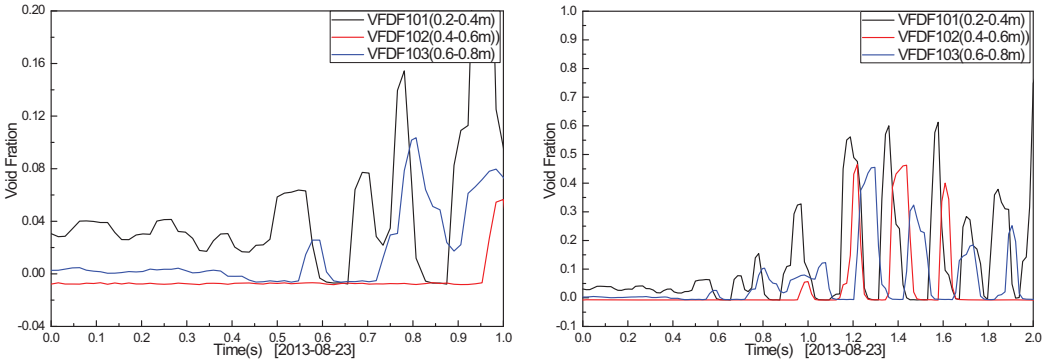

8a. short span 8b. long span

Figure 8. Void Fraction in the TROI76-W4

After the test, the debris was sieved. As shown in Table 3, the total mass obtained from the test section in the TROI30 was 2.2980 kg. The fine debris portion, whose diameter is less than 0.710 mm, is as large as 22% of the whole debris. In the TROI76-W4 where no steam explosion occurred, the fraction of debris of more than 6.35mm is about 40% and the fraction of debris of less than 1mm is about 1.6%. Fig 9. shows the debris after the test. In Fig. 9a, many smaller particles appeared, and one of the side walls was broken because a spontaneous explosion occurred. TROI76-W4 takes a relatively a big portion of the large debris, as shown Fig. 9b, because there was no steam explosion.

Table 3 Results of debris sieving after the tests (ZrO2)

TROI test number	Unit	TROI30	TROI76-W4
Debris Total	[kg]	2.98(100%)	11.916(100%)
>6.35mm	[kg]	0.345(12%)	4.905(41.2%)
4.75mm ~ 6.35mm	[kg]	0.26(9%)	2.715(22.8%)
2.0mm ~ 4.75mm	[kg]	0.875(29%)	3.451(29.0%)
1.0mm ~ 2.0mm	[kg]	0.620(21%)	0.650(5.5%)
0.71mm ~ 1.0mm	[kg]	0.21(7%)	0.095(0.8%)
0.425mm ~ 0.71mm	[kg]	0.26(9%)	0.060(0.5%)
<0.425mm	[kg]	0.4(13%)	0.040(0.3%)


9a. TROI30 9b. TROI76-W4

Figure 9. Debris Picture of ZrO2

3.2. Test using Prototypic Corium

In the TROI68-VISU, the test was carried out with a 1m free fall of the molten corium in air to simulate the partially flooded reactor cavity. The instrumentation of Table 1 was applied. The TROI76-W7 test was carried out to simulate the reactor submerged conditions. Most of the test conditions of the TROI68-VISU and TROI76-W7, as shown in Table 4, are the same except for the injection mode. The square rectangular interaction chamber, a 1m water pool with an inner cross section of 60cm x 60cm, is used to visualize the mixing zone, the melt front velocity in the water, and the water level swell as the melt front reaches the bottom of the interaction chamber.

Table 4 Initial conditions of prototypic corium

TROI test number	Unit	TROI68-VISU (1m Free fall)	TROI79-W7 (w/o Free fall)
Melt UO2/ZrO2	[w/o]	80:20	80:20
Temperature (Max.)	[K]	2,990K	3,015K
Charged mass	[kg]	29.58	34.3
Released mass	[kg]	19.179	22.54
Plug/puncher diameter	[cm]	10.0/8.5	10.0/8.5
Jet diameter	[cm]	5.0(nozzle)	5.0(nozzle)
Nozzle to water surface distance	[m]	1	-0.01
Test Section Water mass	[kg]	360	360
Water pool depth	[cm]	100	100
Cross section	[m2]	0.36	0.36
Initial temperature	[K]	341	341
Pressure Vessel Initial pressure(air)	[MPa]	0.205	0.125
Initial temperature	[K]	307	311

Fig. 10 shows a picture just before the melt reaches the bottom of the interaction chamber of the TROI68-VISU. The time in Fig. 10 is after opening of the valve of the intermediate melt catcher of Fig. 1b. It takes 0.460ms to come out from the valve in the intermediate melt catcher to the exit of the nozzle,

which is located at the same level as the water surface. The average velocity of the melt front passing through the 1m water pool is estimated. The melt front avg. velocity passing through a 1m water pool is about 1.7m/s.

Fig. 11 shows an picture just before the melt reaches the bottom of the interaction chamber of TROI76-W7. The time at Fig. 11 is the time after opening the valve of the intermediate melt catcher. It takes 0.235ms to come out of the valve in the intermediate melt catcher to the exit of the nozzle, which is located at the same level as the water surface. The average velocity of the melt front passing through the 1m water pool is estimated. The average velocity of the melt front is about 2.7 m/s from Fig. 11. A large bubble was also observed on the surface of the mixing zone, which rose up. The mixing zone size is also similar to that in the ZrO2 test.

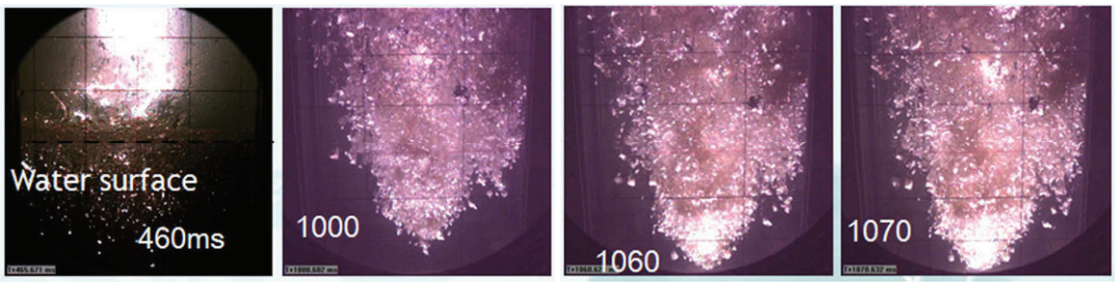

Figure 10. Melt front location with a time in the TROI-VISU

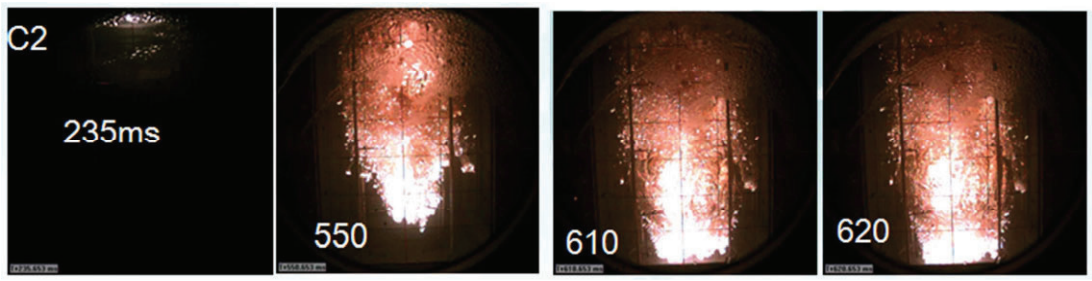

Figure 11. Melt front location with a time in the TROI76-W4

The average velocity of the melt front is also estimated by sacrificial thermo couples, located in the center of the interaction chamber. The average velocity in the TROI68-VISU, as shown in Fig. 12a, is 1.8m/s. This is similar to that estimated by video, i.e., 1.7m/s. The average melt front velocity in the TROI76-W7, as shown in Fig. 12b, is 2.3 m/s. This value is the almost the same as that obtained with a high-speed camera, i.e., 2.7m/s. The result that the melt propagation velocity in the case of submerged m elt release is higher than the one in the case of melt release in a non-submerged case is similar to the ZrO2 case as mentioned above. Even though the initial pressures in the TROI68-VISU and TROI79-W7 are a little different, the system pressures between the furnace vessel where the melt is released and the pressure vessel where the melt interacts with the coolant are the same in each test. Thus, the system pressure difference effect between the furnace vessel and pressure vessel, in other words, when there is a pressure difference between the pressure vessel and cavity, could not be observed in the test.

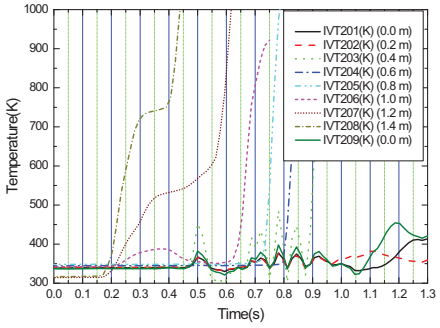

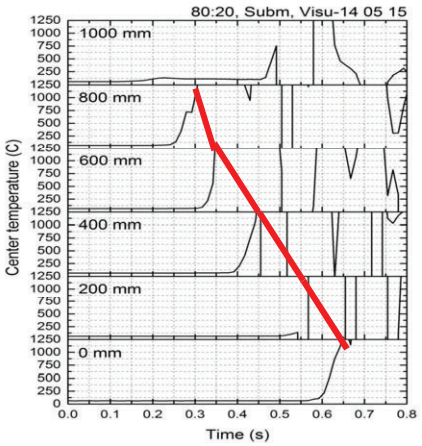

12a. TROI-VISU 12b. TROI- TROI76-W7

Figure 12. Time passing sacrificial thermocouples

The melt velocity with time and/or specific span from the melt injection to the bottom tough can be estimated by using a high-speed camera and/or sacrificial T/Cs, and this information can be used for a code analysis.

The void fraction in the TROI68-VISU, the maximum void fraction before the melt reaches the bottom of the interaction chamber, is about 10% at 0.9 sec, as shown in Fig. 13a. After that, the maximum void fraction from 1.2 sec to 1.4 sec, as shown in Fig. 13b, is about 20% - 40% depending on the location. In the TROI76-W7, the maximum void fraction before the melt reaches the bottom of the interaction chamber is about 2 % at 0.5 sec, as shown in Fig. 14a. The maximum void fraction from 1.2 sec to 1.6 sec, as shown in Fig. 14b, is about 60%-100% depending on the location.

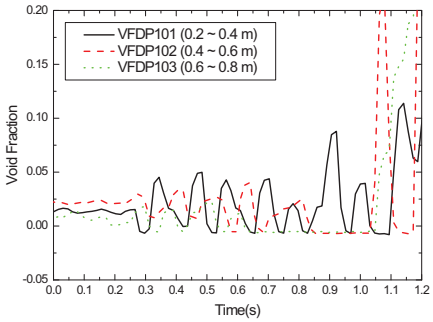

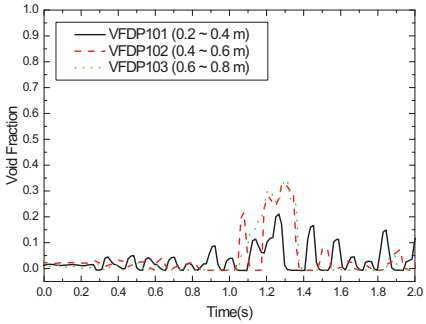

13a. Short span 13b. Long Span

Fig. 13 Void fraction for TROI68-VISU

After the test, the debris was sieved. As shown in Table 5, the fraction of debris of more than 6.35mm in the TROI68-VISU is about 14.7%, and the fraction of debris of less than 1mm is about 10%. The fraction of debris of more than 6.35mm in the TROI76-W4 is about 17% and the fraction of debris of less than 1mm is about 15%. It is difficult to have premixing information from the particle size comparison because some of the particles are produced be passing through the water of the melt jet and some particles can be generated by the impact of the melt jet with the bottom of the interaction chamber. The medium

size debris of 2-4.75mm takes a relatively big portion in the two tests. Fig. 15 shows the debris picture after the test.

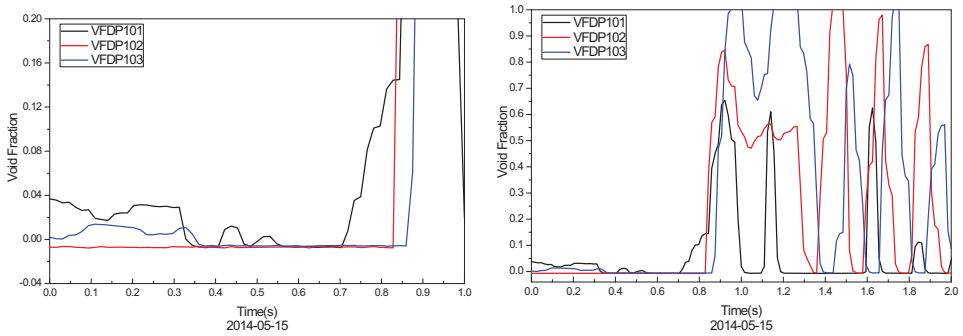

14a. Short span 14b. Long Span

Fig. 14 Void fraction for TROI76-W7

Table 5 Results of debris sieving after the test (Corium)

TROI test number	Unit	TROI68-VISU 1m free fall	TROI79-W7 w/o Free fall
Debris / Total	[kg]	19.179(100%)	22.54(100%)
>6.35mm	[kg]	2.810(14.7%)	3.845(17.1%)
4.75mm ~ 6.35mm	[kg]	3.200(16.7%)	2.030(9.0%)
2.0mm ~ 4.75mm	[kg]	7.955(41.5%)	8.865(39.3%)
1.0mm ~ 2.0mm	[kg]	3.300(17.2%)	4.410(19.6%)
0.71mm ~ 1.0mm	[kg]	0.705(3.7%)	1.245(5.5%)
0.425mm ~ 0.71mm	[kg]	0.680(3.5%)	1.265(5.6%)
<0.425mm	[kg]	0.529(2.8%)	0.88(3.9%)

Figure 15 Debris picture of prototypic corium

4. CONCLUSIONS

The experimental results of simulated FCI under partially flooded reactor cavity conditions and submerged reactor conditions were introduced. The triggered system was not applied for all tests.

- In the FCI test under partially flooded reactor cavity conditions using ZrO2, a spontaneous steam explosion was observed. In the FCI test under the reactor submerged conditions using ZrO2, no spontaneous steam explosion was observed.
- In the FCI test under the partially flooded reactor cavity conditions and under the submerged reactor conditions using corium, no spontaneous steam explosion was observed.
- The melt front velocity in the water under the reactor submerged conditions is much faster than under the partially flooded reactor cavity conditions, and a large bubble during the FCI test under the submerged reactor conditions was observed at the surface of the mixing zone. It seems that the breakup of melt jet in the water during the FCI test under the submerged reactor conditions was not active compared with the FCI test under partially flooded reactor cavity conditions.
- In the FCI test under partially flooded reactor cavity conditions using ZrO2, the fine debris portion whose diameter is less than 0.710 mm is as large as 22% of the whole debris because a spontaneous explosion occurred. In the FCI test under the submerged reactor conditions where there was no steam explosion, the fraction of debris of more than 6.35mm is about 40% and the fraction of debris of less than 1mm is about 1.6%.
- In the FCI tests using corium, there is not much difference in debris size distribution in FCI under the partially flooded reactor cavity conditions and the submerged reactor conditions. This is different than expected because it was expected that a smaller amount of break up would occur due to a large bubble generation: A detailed analysis using the modeling of the breakup length and fragmentation is going to be continued.
- In the experiments, the initial pressure at the melt zone is the same as in the interaction vessel. In other words, the effect of the pressure difference between the pressure vessel and reactor cavity was not considered. The pressure difference may be important for fragmentation in the submerged reactor conditions and could be an area of further work.

ACKNOWLEDGMENTS

This work was supported by the National Research Foundation of Korea (NRF) grant funded by the Korea government (Ministry of Science, ICT, and Future Planning) (No. 2012M2A8A4025889)

REFERENCES

[1] J. H. Song, I. K. Park, Y. J. Chang, Y. S. Shin, J. H. Kim, B. T. Min, S. W. Hong, H. D. KIM, "Experiments on the Interactions of molten ZrO_2 with water using TROI facility", Nuclear Engineering and Design, **213**, pp. 97-110 (2002)

[2] J. H. Song, I. K. Park, Y. S. Shin, J. H. Kim, S. W. Hong, B. T. Min, .H. D. KIM, "Fuel coolant interaction experiments in TROI using a UO_2 /ZrO_2 mixture", Nuclear Science and Engineering A, 357, pp. 297-303 (2003)

[3] J. H. Kim, I. K. Park, B. T. Min, S. W. Hong, Y. S. Shin, J. H. Song and H. D. KIM, "The Influence of Variations in the Water Depth and Melt Composition on a Spontaneous Steam Explosion in the TROI Experiments", '04 ICAPP, Paper # 4010, Pittsburg, USA, 2004 Jun 13-17

[4] J. H. Song, J. H. Kim, S. W. Hong, B. T. Min, H. D. KIM, "The effect of corium composition and interaction vessel geometry on the prototypic steam explosion", Annals of Nuclear Energy, **33**, pp. 1437-1451 (2006)

[5] J. H. Kim, B. T. Min, I. K. Park, S. W. Hong, "Triggered steam explosion with corium melts of various compositions in a narrow interaction vessel in the TROI facility", Nuclear Technology, **169**, pp. 239-251 (2010)

[6] S. W. Hong, Pascal Piluso and Matjaz Leskovar, "Status of the OECD-SERENA project for the resolution of Ex-vessel Steam explosion Risks", Journal of Energy and Power Engineering, **7**, pp. 423-431 (2013)

[7] I. Huhtiniemi, D. Magallon, H. Hohmann, "Results of recent KROTOS FCI tests: Alumina versus corium melts", Nuclear Engineering and Design **189** pp. 379-389 (1999).